Key Engineering Materials Vols. 554-557 (2013) pp 2277-2284

doi:10.4028/www.scientific.net/KEM.554-557.2277

Applying Nagata Patches in the Description of Smooth Tool Surfaces used in Sheet Metal Forming Simulations

D.M. Neto[1,a], M.C. Oliveira[1,b], J.L. Alves[2,c], L.F. Menezes[1,d] and P.Y. Manach[3,e]

[1]CEMUC, Department of Mechanical Engineering, University of Coimbra, Pinhal de Marrocos, 3030-788 Coimbra, Portugal

[2]CT2M, Department of Mechanical Engineering, University of Minho, Campus de Azurém, 4800-058 Guimarães, Portugal

[3]LIMATB, Université Européenne de Bretagne, Université de Bretagne-Sud, BP 92116, 56321 Lorient, France

[a]diogo.neto@dem.uc.pt, [b]marta.oliveira@dem.uc.pt, [c]jlalves@dem.uminho.pt, [d]luis.menezes@dem.uc.pt, [e]pierre-yves.manach@univ-ubs.fr

Keywords: Nagata patch interpolation, Smooth surface description, DD3IMP in-house code, Reverse deep drawing, Experimental and numerical results.

Abstract. This study deals with the new strategy currently implemented in DD3IMP in-house code to describe the forming tools using Nagata patches. The strategy is based on the use of the Nagata patch interpolation to generate smooth contact surfaces over coarse faceted finite element meshes. The description of the adopted algorithm is briefly presented, highlighting the contact search algorithm employed. The reverse deep drawing of cylindrical cups, proposed as benchmark at the Numisheet'99 conference, is selected to examine the accuracy and robustness of the proposed approach. The effect of the gap between the blank-holder and the die is studied, adopting two distinct strategies: fixed gap and variable gap. The numerical results are compared with the experimental ones, previously presented and discussed in [1]. It is shown that the agreement is very good both in terms of punch force evolution and thickness distribution.

Introduction

Nowadays the application of the finite element method in the numerical simulation of sheet metal forming processes plays an important role in the manufacturing industry development. Computer simulation is becoming widely recognized as a low-cost technique used to predict material formability and defects, as well as to optimize process parameters. Thus, several finite element codes have been developed to simulate such processes [2]. Among the in-house codes, DD3IMP is a finite element code that has been specifically developed and optimized to simulate sheet metal forming processes [3], being the one employed in this study. Since it is a fully static implicit code, the equilibrium conditions are check after each increment, which generally assure more accurate results than explicit ones. However, implicit codes are known to be very time-consuming since it is mandatory to solve a system of linear equations in each equilibrium iteration [4].

Concerning the sheet metal forming processes modeling, the forming tools are typically considered as rigid, due to the high difference between their stiffness and the one of the metallic sheet. Thus, only their exterior surfaces are described in the numerical model [5]. The tool surface description method recently adopted in DD3IMP code is based on the use of the Nagata patch interpolation to generate smooth contact surfaces [6,7]. The idea behind this method is to smooth relatively coarse faceted finite element meshes using quadratic Nagata patches. The completely local support of the Nagata patch interpolation, associated with its particular ability to accurately smooth both regular and irregular finite element meshes, are the principal features of this interpolation method [8]. Furthermore, the *quasi*-G^1 continuity between Nagata patches produces a smooth contact surface description, avoiding non-physical jumps in the contact force evolution,

which usually arise when the tool surfaces are discretized by traditional low order finite elements [7,9]. Thus, the Nagata patch description allows attaining a high level of geometric continuity while keeping a low interpolation order, contrary to the typical CAD representations (e.g. NURBS). The approach adopted in the implementation in DD3IMP FEM code of this new strategy to describe the tool surfaces is briefly described in the next section of the paper.

The accuracy and ability of the proposed approach to describe tool surfaces are analyzed in this study through the reverse deep drawing process, proposed as benchmark at the Numisheet'99 conference [10,11]. The results obtained from the numerical simulations carried out with DD3IMP using Nagata patches in the tool surface description are compared with the experimental ones, namely the evolution of the punch force and the thickness distribution in the cup wall.

Forming Tools Described by Nagata Patches

The Nagata patch interpolation is a simple method that can be used to smooth discretized surfaces, recovering their curvature with good accuracy, using only the position and normal vectors at each vertex of the finite element mesh [8,12]. Since any mesh generator allows exporting mesh files containing both the information about the position vector of each mesh vertex and the finite element connectivity, a wide variety of mesh generator packages can be employed. The central idea behind the vertex normal vector evaluation is to use the IGES file format of the original CAD model to perform the projection of each mesh vertex on the corresponding NURBS surface, in order to evaluate the surface partial derivatives and consequently the surface normal vector [13]. Hence, the proposed procedure to describe the forming tools with Nagata patches can be divided in three steps: mesh generation, vertex normal vector evaluation and Nagata patch interpolation [6]. This approach allows the readily creation of new tools using standard mesh files, being the required surface normal vectors extracted from the CAD model by means of the IGES file format, applying the algorithm presented in [13].

The sheet metal forming processes involve several forming tools, presenting dissimilar geometries. Therefore, each tool must be described by a set of Nagata patches, which corresponds to the number of faceted finite elements resulting from the discretization of the tool surfaces. The number of patches required for the proper description of each tool increases with its geometric complexity. Previous studies report the accuracy of the interpolation applied to simple geometries, evaluating the maximum shape error for different mesh refinements. The results show that the interpolation convergence of the traditional faceted finite element approximation is quadratic regardless of the geometry. On the other hand, the Nagata patch interpolation always attains a higher order of convergence, which varies from quartic (cylinder, cone and sphere) to nearly cubic (torus) [6,8].

Contact Search Algorithm. Sheet metal forming processes involve large slips between the sheet and the forming tools, which must be taken into account in the numerical modeling. Thus, since the configuration of the sheet may change somewhat arbitrarily during the process evolution, any contact node can come into contact with any patch describing the tools. The aim of the contact search algorithm is to quickly detect all the possible candidate contact nodes, at each increment of displacement. Therefore, the contact searching needs to be both efficient and accurate in order to identify all potential contact zones. The contact search algorithm used to deal with the Nagata patches is divided into a global and local search procedure [14].

The global search algorithm identifies all potential contact patches, while the local contact search algorithm evaluates the position where the contact node can eventually establish contact and, simultaneously, determines the contact kinematic variables necessary to the contact enforcement. The global contact search algorithm currently implemented in the DD3IMP code can be divided into the following steps, performed for each contact candidate node: (i) selection of a reduced number of closest tool mesh vertices and application of inverse mesh connectivity to extract their corresponding contact candidate patches; (ii) creation of a uniform grid of points on each of the selected patches, and (iii) selection of the 10 closest Nagata patches for local contact search, based

on the minimum distance between the contact node and the grid of points. Since the contact discretization scheme employed in the DD3IMP code is the widely used node-to-segment approach [14], the local contact search comprises the identification of a point on the selected patch that minimizes the distance to the contact node. The orthogonal projection algorithm is adopted to determine the position vector of the point where contact can be established [7].

Reverse Deep Drawing Process

The increasing computational capacity over the last years allows the numerical simulation of more complex forming processes, such as multi-stage processes and trimming operations classically involved, as well as the optimization of the process conditions at each stage [4]. However, within the framework of the numerical modeling, several aspects can still be improved to decrease the discrepancy between experimental and numerical results, particularly in multi-stage drawing. This type of process is used when a single-stage drawing operation is not sufficient to attain the required drawing ratio. Typically, the forming process is decomposed into two or more stages in order to increase the material formability [1,15,16]. Among the variants of the multi-stage drawing process, the reverse redrawing process is well-known by allowing increased formability when compared with the forward redrawing process. The reverse redrawing process is characterized by the inversion of the drawing direction between the first and the second stage. Thus, the outside of the part during the first stage becomes the inside of the part in the second stage. Since the stress and thickness distribution resulting from the first stage will influence the succeeding stage, its modeling is even more difficult than the single-stage drawing. Moreover, the occurrence of important strain path changes during the second stage requires to use constitutive laws able to describe the mechanical behavior, when submitted to such changes, which are typically more complex [17,18]. The reverse deep drawing of a cylindrical cup, proposed as benchmark at the Numisheet'99 conference [10], is the one considered in this study to validate the accuracy, robustness and ability of the new method employed to describe the forming tools.

Experimental Procedure. The experimental device used to perform the reverse deep drawing process was implemented in a classical electromechanical tensile test machine of maximum capacity of 100 kN. The blank sheet, with an initial diameter of 170 mm, is firstly drawn into a cylindrical cup with 100 mm internal diameter and then into a cup with 73.4 mm internal diameter in the reverse way, as shown in Fig. 1 (a) [10].

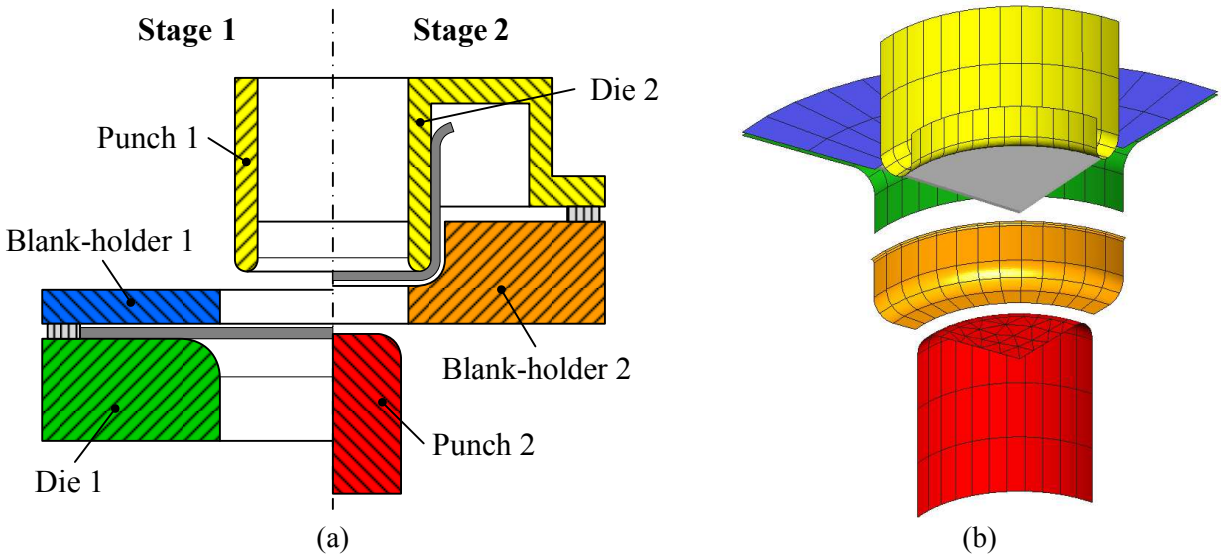

Figure 1: Reverse deep drawing process: (a) schematic drawing for stage 1 (left-hand side) and stage 2 (right-hand side); (b) tool surfaces described by Nagata patches and blank at initial position.

Table 1: Main dimension of the tools for both stages [mm].

Tool geometry	Stage 1	Stage 2
Die opening diameter	104.5	78.0
Die radius	8.0	5.5
Die height	21.0	16.0
Punch diameter	100.0	73.4
Punch radius	5.5	8.5
Blank-holder opening diameter	104.5	105.0
Blank-holder radius	-	7.0
Blank-holder height	-	20.0

Table 2: Material parameters for the work hardening Swift law and Hill'48 yield criterion.

Material parameter	Value
Y_0 [MPa]	180.3
K [MPa]	555.3
n	0.208
F	0.314
G	0.366
H	0.634
$L=M$	1.500
N	1.176

The material adopted in the present study is a DDQ mild steel, supplied with a thickness of 0.98 mm. The main dimensions of the tools for both drawing stages are given in Table 1. The blank-holder is connected to the die by using sixteen screws regularly spaced, introducing adjustable keys to control the gap between the blank-holder and the die. The gap is held fixed in both stages. The value of the gaps was determined in order to draw a cup without wrinkles, being set equal to 1.0 mm in stage 1 and 1.4 mm in stage 2. The punch stroke in stage 1 is defined to be 48.3 mm and for stage 2 is 69 mm. The blank was lubricated (Fuchs 4107S) on both sides at the beginning of each stage. The evaluated experimental data for both stages are the punch force evolution and the thickness distribution in the cup height at 0º, 45º and 90º to the rolling direction (RD) [1,17].

Numerical Modeling. The numerical simulations of the reverse deep drawing process are carried out using the DD3IMP in-house finite element code [3], which uses an updated Lagrangian scheme to integrate the constitutive law in an implicit way. The Coulomb law describes the contact with friction, being the contact constraints enforced through an augmented Lagrangian approach.

Due to geometric and material symmetry conditions, only one quarter of the model is simulated, as shown in Fig. 1 (b). The total number of Nagata patches applied in the tool surfaces description is 354, employing both triangular and quadrilateral patches (see punch 2 in Fig. 1 (b)). This number of patches ensures a shape error inferior to 0.04 mm, being this value very small when compared with the main dimensions of the tools, presented in Table 1. Note that the flat zones when described by Nagata patches present null error. The circular blank (only one-quarter) is discretized with 8-node hexahedron solid finite elements combined with a selective reduced integration technique. The total number of solid elements is 10494, using 2 layers of elements through the thickness. The elastic properties of the mild steel are defined as $E = 200\,\text{GPa}$ and $\nu = 0.3$. Although more complex hardening models could be adopted [17], in this work the isotropic work-hardening is assumed to be described by a Swift law:

$$\sigma = K(\varepsilon_0 + \bar{\varepsilon}^{\text{p}})^n \quad \text{with} \quad \varepsilon_0 = (Y_0/K)^{1/n}, \tag{1}$$

where $\bar{\varepsilon}^{\text{p}}$ is the equivalent plastic strain. The material parameters K, n and Y_0 are presented in Table 2, which are evaluated using only the mechanical properties provided by the benchmark committee and indicated in Table 3. In this work, the anisotropic behavior of the mild steel is described with the Hill's 1948 yield criterion. The Hill's coefficients presented in Table 2 are calculated from the r-values at 0º, 45º and 90º to the RD, provided in Table 3. The friction coefficient between sheet and tools is taken from the benchmark specifications as $\mu = 0.15$.

Since the process is decomposed into two stages, between them, both the blank-holder 1 and die 1 are numerically removed to perform the second stage, in accordance with the experimental procedure. In order to avoid convergence problems when the cup rim comes into contact with the blank-holder 2, a fillet radius of 1.0 mm is introduced between the vertical and horizontal wall, as shown in Fig. 1 (b). Concerning the first stage, the effect of the blank-holder modeling on the

numerical results is studied, applying distinct gaps between it and the die. Indeed, this parameter is particularly important when large contact forces arise on the blank-holder, which can lead to its elastic deflection depending on the clamping system and its rigidity.

Table 3: Mechanical properties of DDQ mild steel provided by the benchmark committee.

Orientation to RD	Yield Strength [MPa]	Tensile Strength [MPa]	*n*	*r* ratio
0º	176	322	0.214	1.73
45º	185	333	0.203	1.23
90º	180	319	0.206	2.02

Results and Discussion

While the gap between the die and the blank-holder was considered constant in stage 2 (1.4 mm), at the stage 1 two models were built using different approaches to numerically control the gap, always taking into account the value imposed experimentally (1.0 mm). Hence, the first model uses a fixed gap of 1.13 mm, which was selected before in [1] to better fit the numerical and experimental force-displacement results. Nevertheless, the results obtained in the current study indicate that the coarse finite element mesh adopted to model the blank in that previous study may have led to an overestimated value of the contact forces. Therefore, a second model was built considering a variable gap between the die and the blank-holder, which is a function of the punch displacement. Fig. 2 (a) presents the evolution of the imposed gap with the punch displacement, used in each model. While the gap is held fixed in the first model, the variable gap applied in the second model is divided into six linear fragments, being its range from 1.0 mm at the beginning of the process until a maximum value of 1.12 mm for a punch displacement of 38.5 mm. This evolution was selected in order to take into account the possible deflection of the blank-holder, which results from the combination of the selected clamping system (through screws) and the high contact forces involved in the process. Its profile follows the shape of the blank-holder force evolution for the fixed gap case. The resultant blank-holder force evolution is presented in Fig. 2 (b) for each model adopted. Since the gap between the die and the blank-holder in the model "Variable gap" is always inferior to the fixed value used in the "Fixed gap" model, the resulting blank-holder force is always higher in the "Variable gap" model. The computational time spent to carry out the complete numerical simulation using a fixed gap was about two hours, while applying a variable gap leads the computational time to about four hours and half. The increase in computational time derives both from the updating of tool position and the higher value of contact forces attained near to 40 mm of punch displacement.

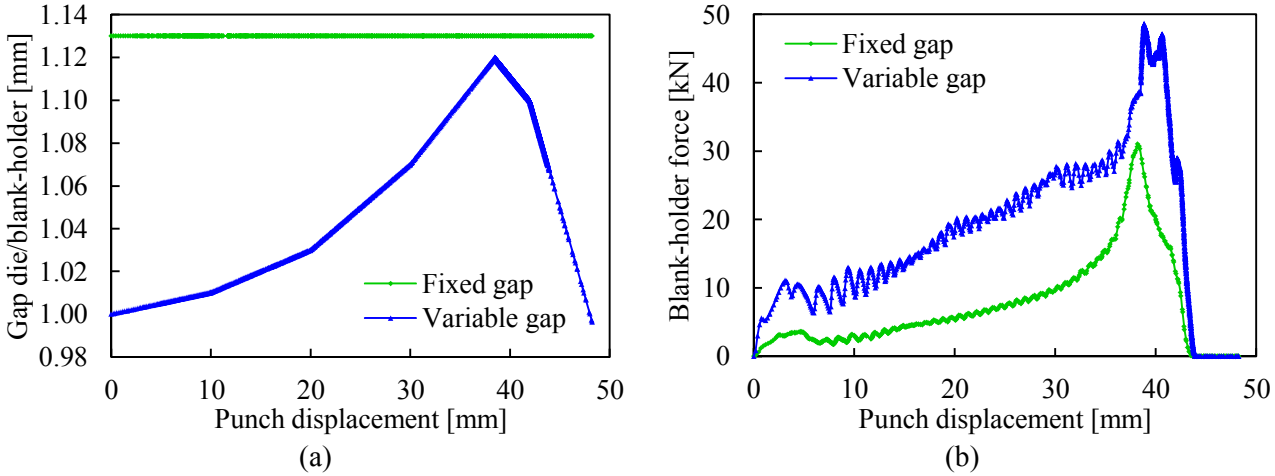

Figure 2: Numerical evolution of the: (a) gap between the die and the blank-holder as a function of the punch displacement; (b) blank-holder force with the punch displacement, both for stage 1.

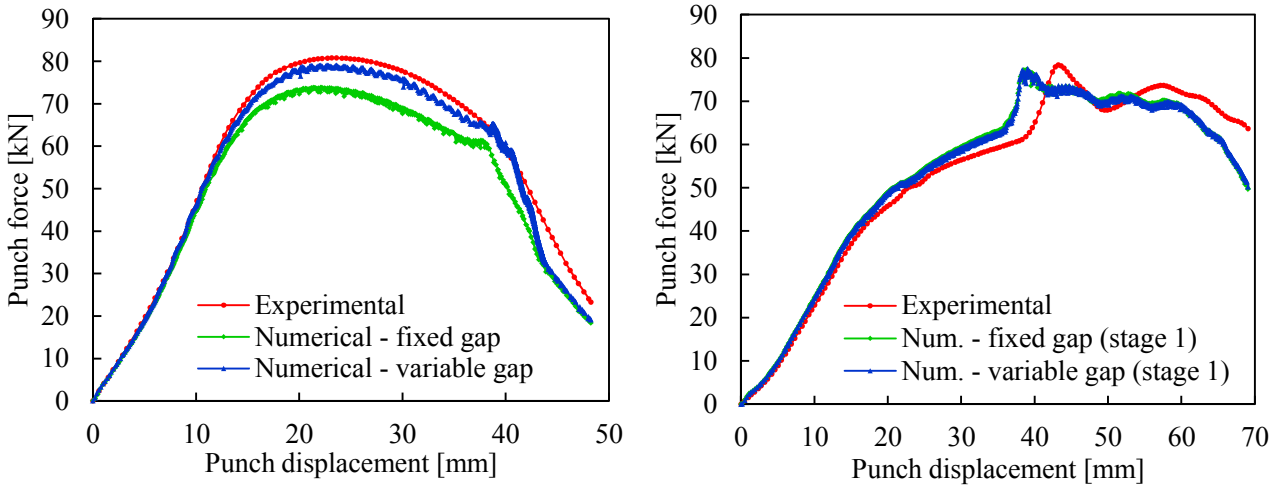

Figure 3: Comparison between experimental and numerical punch force-displacement evolution for: (a) stage 1; (b) stage 2.

The evolution of the punch force with its displacement during the first and second stage is plotted in Fig. 3 (a) and Fig. 3 (b), respectively. Concerning stage 1, the numerical predictions underestimate the force level whatever the gap between die and blank-holder selected. However, the application of the variable gap gives a punch force evolution closer to the experimental data. Therefore, it is concluded that the structural stiffness of the blank-holder used in the experimental device is not suitable to consider a fixed gap in the numerical model.

The prediction of the punch force evolution in stage 2 is only slightly affected by the gap distribution selected for stage 1, as shown in Fig. 3 (b). The numerically predicted punch force evolution overestimates slightly the experimental data until 40 mm of punch displacement and underestimates after 50 mm of displacement. The experimental force exhibits a peak for a punch displacement around 45 mm, which is associated with passage of the cup rim between the die and the blank-holder. This tendency is also numerically reproduced, although it occurs for a lower punch stroke value. This discrepancy can be explained with the ears amplitude, mainly the excessive draw-in predicted numerically at 45º to the RD (see Fig. 4 (a)), which drives the beginning of the force peak. Fig. 4 (a) and (b) show the final shape of the cups at the end of both stages, showing that the cups are not fully drawn for the total punch displacement. The figure also shows the equivalent plastic strain distribution at the end of both stages, being its maximum value of approximately 0.57 in stage 1 and 1.22 in stage 2. The results of Fig. 4 as well as all the others presented in the following analysis correspond to the "Variable gap" model since it allows a more accurate prediction of the punch force evolution.

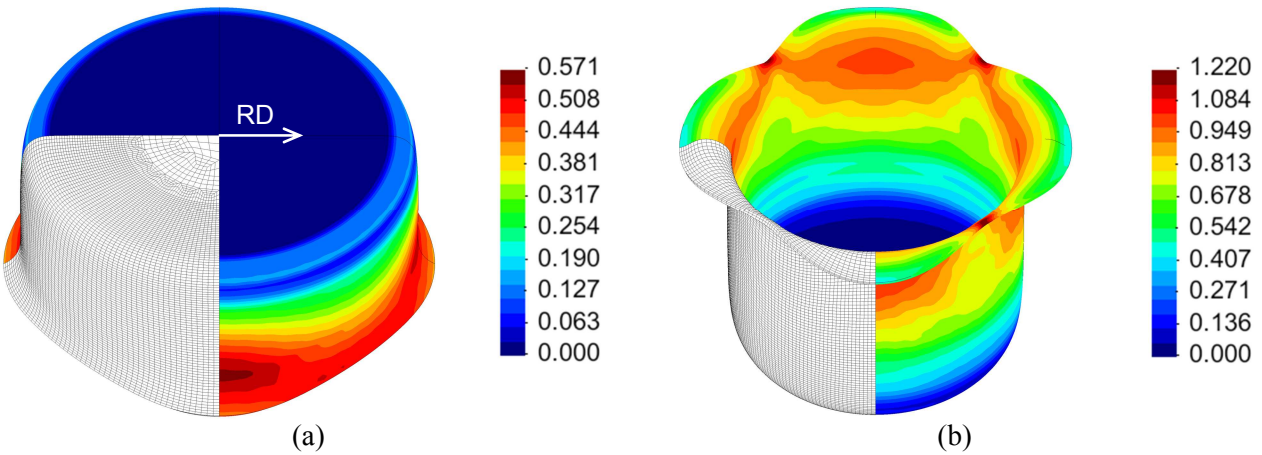

Figure 4: Equivalent plastic strain distribution and deformed mesh at the end of: (a) stage 1; (b) stage 2.

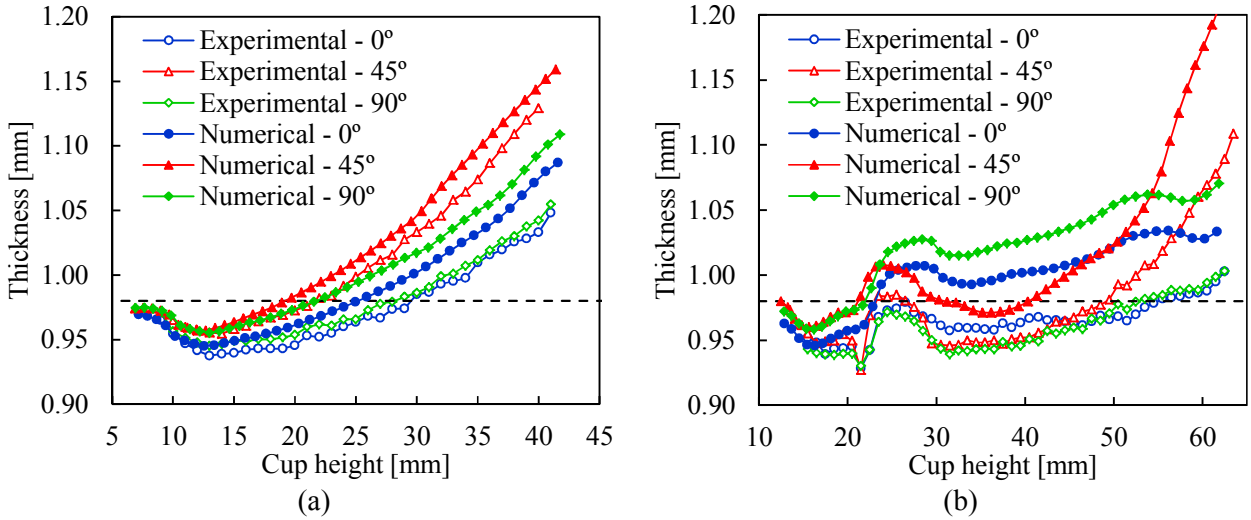

Figure 5: Comparison between experimental and numerical results for the thickness distribution along cup wall after: (a) stage 1; (b) stage 2.

The comparison between experimental and numerical thickness profiles in the cup wall is presented in Fig. 5 for the end of each stage at 0º, 45º and 90º to the RD. The results are shown until a cup height of approximately 42 mm in stage 1 and 63 mm in stage 2. Fig. 5 (a) shows that thickness is overestimated in the three directions during the first stage and the same tendency is observed in Fig. 5 (b) for the second stage. The discrepancy increases with the cup height in stage 1, while in stage 2 it remains constant for cup heights over 30 mm, being the highest difference observed at 90º to the RD. The maximum difference attained in the thickness at the end of stage 1 is around 4%, while that for stage 2 is around 7%.

Conclusions

The new strategy recently implemented in DD3IMP in-house code to describe smooth tool surfaces applying Nagata patches is successfully validated using the reverse deep drawing process. A brief description of the algorithms employed to deal with the new tool description is presented, focusing on the adopted contact search algorithm and the required inputs for the smoothing method. These algorithms allow the numerical simulation of the complex reverse deep drawing without any user intervention, although the code adopted is fully implicit. Both punch force evolution and thickness profiles in the cup wall are presented and compared with the experimental results discussed previously [1]. Two distinct strategies are used to define the gap between the die and the blank-holder in the first stage. Imposing the gap as a function of the punch displacement, the predicted force-displacement evolution is very close to the experimental one in the stage 1, being the force evolution in stage 2 not affected. In addition, the experimental force peak that occurs in stage 2 is numerically reproduced, though for a lower punch stroke. Concerning the thickness predictions, the tendency of the thickness along the cup height is numerically reproduced, despite being overestimated with maximum difference with the experimental results of 7%.

Acknowledgements

The authors gratefully acknowledge the financial support of the Portuguese Foundation for Science and Technology (FCT) under Project PTDC/EME-TME/103350/2008 by FEDER through the program QREN (COMPETE: FCOMP-01-0124-FEDER-010301). The first author is also grateful to the FCT for the PhD grant SFRH/BD/69140/2010.

References

[1] S. Thuillier, P.Y. Manach, L.F. Menezes, M.C. Oliveira, Experimental and numerical study of reverse re-drawing of anisotropic sheet metals, J. Mater. Process. Technol. 125-126 (2002) 764-771.

[2] A. Makinouchi, Sheet metal forming simulation in industry, J. Mater. Process. Technol. 60 (1996) 19-26.

[3] L.F. Menezes, C. Teodosiu, Three-dimensional numerical simulation of the deep-drawing process using solid finite elements, J. Mater. Process. Technol. 97 (2000) 100-106.

[4] L.F. Menezes, D.M. Neto, M.C. Oliveira, J.L. Alves, Improving Computational Performance through HPC Techniques: case study using DD3IMP in-house code, AIP Conf. Proc. 1353 (2011) 1220-1225.

[5] A. Santos, A. Makinouchi, Contact strategies to deal with different tool descriptions in static explicit FEM of 3-D sheet-metal forming simulation, J. Mater. Process. Tech. 50 (1995) 277-291.

[6] D.M. Neto, M.C. Oliveira, L.F. Menezes, J.L. Alves, Improving Nagata patch interpolation applied for tool surface description in sheet metal forming simulation, Comput.-Aided Des. 45 (2013) 639-656.

[7] D.M. Neto, M.C. Oliveira, L.F. Menezes, J.L. Alves, Applying Nagata patches to smooth discretized surfaces used in 3D frictional contact problems: submitted to Comput. Method Appl. Mech. Eng. (2013).

[8] T. Nagata, Simple local interpolation of surfaces using normal vectors, Comput. Aided Geom. Des. 22 (2005) 327-347.

[9] V. Padmanabhan, T.A. Laursen, A framework for development of surface smoothing procedures in large deformation frictional contact analysis, Finite Elem. Anal. Des. 37 (2001) 173-198.

[10] Numisheet 1999, Benchmark C reverse deep drawing of a cylindrical cup, in: J.C. Gelin, P. Picard (Eds.), Numisheet'99 - The 4th International Conference and Workshop on Numerical Simulation of 3D Sheet Forming Processes, Besançon, 1999, pp. 871-932.

[11] J. Danckert, K.B. Nielsen, P. Hojbjerg, Experimental investigation of Numisheet'99 benchmark test C, in: J.C. Gelin, P. Picart (Eds.), Numisheet'99 - The 4th International Conference and Workshop on Numerical Simulation of 3D Sheet Forming Processes, Besançon, France, 1999, pp. 637-642.

[12] T. Hama, T. Nagata, C. Teodosiu, A. Makinouchi, H. Takuda, Finite-element simulation of springback in sheet metal forming using local interpolation for tool surfaces, Int. J. Mech. Sci. 50 (2008) 175-192.

[13] D.M. Neto, M.C. Oliveira, L.F. Menezes, J.L. Alves, Nagata patch interpolation using surface normal vectors evaluated from the IGES file: submitted to Finite Elem. Anal. Des. (2012).

[14] J.O. Hallquist, G.L. Goudreau, D.J. Benson, Sliding interfaces with contact-impact in large-scale Lagrangian computations, Comput. Methods Appl. Mech. Eng. 51 (1985) 107-137.

[15] S.K. Esche, M.A. Ahmetoglu, G.L. Kinzel, T. Altan, Numerical and experimental investigation of redrawing of sheet metals, J. Mater. Process. Technol. 98 (2000) 17-24.

[16] D.K. Min, B.H. Jeon, H.J. Kim, N. Kim, A study on process improvements of multi-stage deep-drawing by the finite element method, J. Mater. Process. Technol. 54 (1995) 230-238.

[17] S. Thuillier, P.Y. Manach, L.F. Menezes, Occurrence of strain path changes in a two-stage deep drawing process, J. Mater. Process. Technol. 210 (2010) 226-232.

[18] J.W. Yoon, F. Barlat, R.E. Dick, K. Chung, T.J. Kang, Plane stress yield function for aluminum alloy sheets-part II: FE formulation and its implementation, Int. J. Plast. 20 (2004) 495-522.